PHYSICAL REVIEW D **78,** 063530 (2008)

CMB and 21-cm signals for dark matter with a long-lived excited state

Douglas P. Finkbeiner,[1] Nikhil Padmanabhan,[2] and Neal Weiner[3]

[1]*Harvard-Smithsonian Center for Astrophysics, 60 Garden Street, Cambridge, Massachusetts 02138, USA*
[2]*Physics Division, Lawrence Berkeley National Laboratory, 1 Cyclotron Road, Berkeley, California 94720, USA*
[3]*Center for Cosmology and Particle Physics, Department of Physics, New York University, New York, New York 10003, USA*

(Received 12 June 2008; published 18 September 2008)

Motivated by the eXciting dark matter model of Finkbeiner and Weiner, hypothesized to explain the 511 keV signal in the center of the Milky Way, we consider the cosmic microwave background and 21-cm signatures of models of dark matter with collisional long-lived excited states. We compute the relic excitation fraction from the early Universe for a variety of assumptions about the collisional de-excitation cross section and thermal decoupling. The relic excitation fraction can be as high as 1% for natural regions of parameter space, but could be orders of magnitude smaller. Since the lifetime of the excited state is naturally greater than 10^{13} s, we discuss the signatures of such relic excitation on cosmic microwave background and high-z 21-cm observations. Such models have potentially richer astrophysical signals than the traditional weakly interacting massive particle annihilations and decays, and may have observable consequences for future generations of experiments.

DOI: 10.1103/PhysRevD.78.063530 PACS numbers: 95.35.+d

I. INTRODUCTION

To explain the apparent excess of $e^{\pm}$ annihilation in the galactic bulge observed by the INTErnational Gamma-Ray Astrophysics Laboratory (INTEGRAL) [1,2], Finkbeiner and Weiner [3] proposed a model of eXciting dark matter (XDM) in which weakly interacting massive particles (WIMPs) collisionally excite and subsequently de-excite via $e^{\pm}$ emission. This model uses the kinetic energy of the WIMP dark matter to create $e^{\pm}$ pairs, in contrast with light dark matter models in which the pairs result from the mass energy of WIMP annihilation (e.g., [4]), where the WIMP mass must be less than a few MeV [5,6]. Because the XDM WIMP must have a weak-scale mass (~ 500 GeV), it retains many of the desirable properties of weak-scale WIMPs such as the thermal relic freeze-out abundance.

The lifetime of such an excited state need not be short, and indeed, could be of order the age of the Universe today. This raises the possibility of a long-lived relic excited fraction with observable consequences. A simple argument shows the large amount of energy potentially available from de-excitations—assuming 100% of the dark matter (DM) is the XDM WIMP, and the relic excitation fraction is Y_f, the energy per baryon, p, is

$$p = Y_f \eta M_\chi \frac{n_\chi}{n_b} = Y_f \eta \frac{\rho_{\rm DM}}{\rho_b} m_p, \tag{1}$$

where η is the fraction of the WIMP mass converted to kinetic energy by the de-excitation, M_χ is the WIMP mass, and $\rho_{\rm DM}/\rho_b \approx 5$. For the fiducial XDM model, we take

$$\eta = (\delta - 2m_e)/M_\chi, \tag{2}$$

which for mass splitting $\delta \approx 1.1$–2 MeV, and $M_\chi =$ 500 GeV yields $\eta \approx 2 \times 10^{-7}$ to 2×10^{-6}, or

$$p \approx Y_f (1\text{–}10 \text{ keV/baryon}). \tag{3}$$

This amount of energy, even if inefficiently transferred to the gas, could completely ionize the Universe many times over for $Y_f = 1/2$. For the more realistic case of $Y_f \ll 1/2$, the consequences depend on when and where the energy is deposited, and with what efficiency.

This paper explores the astrophysical phenomenology of XDM WIMP relic excitations. We start by showing that for a natural range of cross sections, the residual excited fraction can be high enough ($> 10^{-4}$) to have measurable consequences. We then explore these consequences, focusing on the ionization and thermal history of the Universe, and discuss how observations of the cosmic microwave background and diffuse 21-cm radiation might constrain such effects. Our goals here are two-fold: to determine whether the specific model of XDM proposed to explain the 511 keV excess is constrained by other astrophysical probes, and to explore more generally the phenomenology of a WIMP with one or more excited states. As we shall show, this more general class of "XDM"-like models could have a much richer astrophysical phenomenology than traditional WIMPs.

II. KINETIC DECOUPLING AND DECAYS OF XDM PARTICLES

Before addressing the implications of excited states on reionization, we must address two questions within the context of the model: how does the kinetic temperature of the XDM relate to the photon temperature when de-excitation goes out of equilibrium, and what is the lifetime of the excited state χ^*? The former question is important for determining the precise value of the relic density of χ^*, while the latter is important for the transfer of energy from the χ^* to ionization in the later universe.

A. Summary of the XDM model

The defining feature of the XDM model is that the WIMP has an excited state, which can be collisionally excited, and subsequently decay to e^+e^- pairs. The excited state could exist due to compositeness of the dark matter, or arise from an approximate symmetry of the theory.

For the excited state to be accessible in the Milky Way, and relevant for e^+e^- production, only a narrow kinematical range must be considered for the mass splitting, δ. For the decay to the ground state to be energetically capable of producing e^+e^- pairs, one must have $\delta > 1.022$ MeV. On the other hand, the kinetic energy available for a pair of 500 GeV WIMPs colliding each with velocities $v \sim 600$ km/s (roughly the escape velocity of the Galaxy), is 2 MeV, setting an upper bound on δ.

To produce a sufficiently high number of positrons to explain the INTEGRAL signal, a large cross section is required [3,7], comparable to the geometric cross section set by the characteristic momentum transfer. That is, $\sigma \sim (M_\chi \delta)^{-1}$ is of the correct size. Such a cross section can arise naturally [3], but requires the presence of a new light scalar ϕ, with $m_\phi^2 \lesssim M_\chi \delta$. The χ can excite by emitting a ϕ with amplitude λ_- or can scatter elastically with amplitude λ_+. We generally assume $\lambda_- \sim \lambda_+$, but this is not necessary.

Most of the equilibrium properties relevant to our discussion here are ultimately set by the interactions of ϕ, which stays in thermal equilibrium with the standard model through its mixing with the Higgs. Thus, the most relevant term for the discussion at hand is the ϕ-Higgs coupling

$$\mathcal{L} \supset \alpha \phi^2 h^\dagger h. \tag{4}$$

When the Higgs acquires a vacuum expectation value (VEV), this contributes to the mass of the ϕ. Thus requiring a tuning better than 1% in parameters yields a naturalness upper bound of about $\alpha \lesssim 10^2 m_\phi^2/v^2 \sim 2 \times 10^{-3}(m_\phi^2/1\ \mathrm{GeV}^2)$. Assuming a VEV $\langle\phi\rangle \sim m_\phi$, one finds a mixing angle between the ϕ and Higgs of $\sin\theta \approx \alpha m_\phi v/m_h^2 \lesssim 10^{-4}$ [8]. Note that the natural range of mixing angle is correlated with m_ϕ. That is, since $\alpha \lesssim 10^2 m_\phi^2/v^2$, $\sin\theta \lesssim 10^2 m_\phi^3/(100\ \mathrm{GeV})^3$. Thus, very light ϕ's are naturally more weakly mixed than heavier ϕ's.

B. Kinetic Decoupling of XDM

Although XDM annihilation $\chi\chi \leftrightarrow \phi\phi$ freezes out in a fashion similar to usual WIMPs at $T \sim M_\chi/20$, kinetic decoupling is a somewhat more subtle story. Direct elastic scattering $\chi f \to \chi f$ is both Yukawa and mixing suppressed, and is thus inefficient at maintaining kinetic equilibrium.

The dominant process contributing to kinetic equilibrium of χ is $\chi\phi \to \chi\phi$ shown in Fig. 1. The scattering

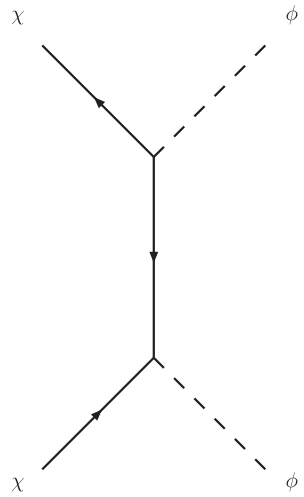

FIG. 1. Dominant diagram contributing to kinetic equilibrium of χ.

cross section for this process is

$$\sigma = \frac{\lambda^4}{4\pi m_\phi^2}, \tag{5}$$

where λ is the $\chi - \chi - \phi$ coupling. (We assume $\lambda_+ \sim \lambda_-$ here for simplicity, although that does not significantly change this discussion. Additionally, we do not distinguish between χ and χ^* at this temperature $T \gg \delta$.) With such a cross section and $\lambda \sim 0.1$, assuming a thermal presence of ϕ, χ will remain in kinetic equilibrium down to $T \simeq m_\phi/30$.

Ultimately, the relevant process for determining the decoupling temperature is when ϕ decouples from the thermal bath. The dominant diagram for this process is shown in Fig. 2. Since we are principally interested in the lowest possible temperature T_{dec}, we are interested in the

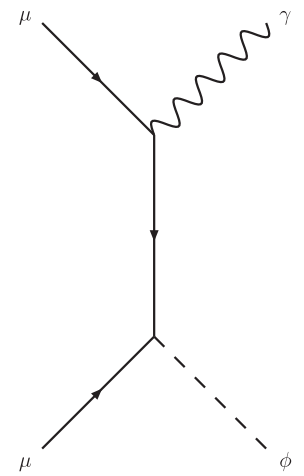

FIG. 2. Dominant diagram contributing to thermal equilibrium of ϕ.

situation where the fermion in question is a muon, and the cross section (for relativistic μ and nonrelativistic ϕ) is approximately given by

$$\sigma = \frac{y_\mu^2 \sin^2\theta \alpha_{\rm em}}{8\pi m_\phi^2}, \tag{6}$$

where $\alpha_{\rm em}$ is the fine structure constant.

Such a scattering can keep the ϕ in equilibrium down to below the muon mass for $\sin\theta = 10^{-4}$, while for smaller mixings the temperature of decoupling is higher (roughly 1 GeV for $\sin\theta = 10^{-5}$, where additional fields, such as pions and kaons, are relevant). As such, we limit ourselves to the range of $T_{\rm dec} > 100$ MeV, although one could conceivably stay in equilibrium longer in other models.

C. Lifetime

In addition to the couplings that drive the early thermal history, the lifetime of both χ^* and ϕ are clearly important. The lifetime of χ^* is crucial, because this determines when the energy of the excited state can be deposited into the baryonic gas of the early Universe. The lifetime of ϕ is important, as we have ignored its presence in the calculations at $T \approx 1$ MeV, and we need to see that this is justified.

We begin by considering the lifetime of the χ^*. Both excited and unexcited states of the dark matter will come into thermal equilibrium in the early Universe, with the excited state decaying into the lighter state with an approximate lifetime

$$\tau_{\chi^*} \approx 10^{15}\ {\rm s} \left(\frac{0.1}{\lambda_-}\right)^2 \left(\frac{10^{-4}}{\sin\theta}\right)^2 \left(\frac{1\ {\rm MeV}}{\sqrt{\delta^2 - 4m_e^2}}\right)^5 \left(\frac{m_\phi}{1\ {\rm GeV}}\right)^4. \tag{7}$$

Consequently, for the parameters under consideration, lifetimes in the range of 10^{13} s to 10^{18} s are quite reasonable.

Although it appears one can make the lifetime much longer simply by lowering m_ϕ, there is an implicit link between m_ϕ and $\sin\theta$ because of naturalness. Lower values of m_ϕ may quickly lead to a highly tuned region of parameter space.

The scalar ϕ decays through its mixing with the Higgs, and thus has a lifetime

$$\tau_\phi = \sin^{-2}\theta \tau_h(m_h = m_\phi). \tag{8}$$

That is, the lifetime of ϕ is just $\sin^{-2}\theta$ times that of a Higgs boson with mass m_ϕ. This decay is typically dominated by a single process. For example, for $m_\phi \lesssim 1$ MeV, the ϕ decays into $\gamma\gamma$. A Higgs of this mass has a lifetime $\tau \sim 3 \times 10^{-4}$ s [9]. Thus, the ϕ will have a lifetime $\tau_\phi \sim 3\sin^{-2}\theta \times 10^{-4}$ s. Although such extremely light ϕ bosons are potentially interesting, they occupy a very tuned region of parameter space.

For $2m_e \lesssim m_\phi \lesssim 2m_\mu$, $\phi \to e^+e^-$ dominates, and the ϕ lifetime will range $10^{-9}\sin^{-2}\theta \lesssim \tau_\phi/(1\ {\rm s}) \lesssim 3 \times 10^{-11}\sin^{-2}\theta$. Thus, for mixing angles $\sin\theta \sim 10^{-4}$, such particles would decay before nucleosynthesis, and in general well before kinetic decoupling of χ. The most natural region of parameter space (with the lowest tuning), $2m_\mu \lesssim m_\phi \lesssim 1$ GeV, $\phi \to \mu^+\mu^-$, and $\phi \to \pi\pi$ become available, and the ϕ lifetime will range $3 \times 10^{-15}\sin^{-2}\theta \lesssim \tau_\phi/(1\ {\rm s}) \lesssim 3 \times 10^{-18}\sin^{-2}\theta$. In this range of parameters, ϕ will have certainly decayed before kinetic decoupling of χ.

Thus, with reasonable values for the mixing parameter, we find the scalar is relatively short-lived. However, the decay of the excited state χ^* into the lighter state χ will naturally occur late in the Universe, producing positrons and feeding energy into the baryonic fluid. The amount of energy will depend directly of the number of relic χ^*'s left over from the big bang.

III. COLLISIONAL XDM FREEZE-OUT

Excitation and de-excitation of the WIMP proceeds at rates k_E and k_D, respectively, via reactions of the form

$$\chi\chi \leftrightarrow \chi^*\chi, \tag{9}$$

$$\chi\chi^* \leftrightarrow \chi^*\chi^*. \tag{10}$$

For simplicity, we assume that the rates for both channels (9) and (10) are equal, and neglect double excitations and double de-excitations. We denote the physical (not comoving) densities of χ, χ^* by n_χ, n_{χ^*} and define $n \equiv n_\chi + n_{\chi^*}$. The Boltzmann equation for n_{χ^*} is then

$$\frac{dn_{\chi^*}}{dt} + 3H(t)n_{\chi^*} = -k_D n_{\chi^*} n + k_E n_\chi n, \tag{11}$$

where $H(t)$ is the Hubble constant at time t. Defining $Y \equiv n_{\chi^*}/n$ and a dimensionless inverse temperature $x \equiv \delta/T$, this simplifies to

$$\frac{dY}{dt} = -k_D n[Y - (1 - Y)f(x)e^{-x}], \tag{12}$$

where

$$f(x) = \sqrt{1 + \frac{\pi x}{4}}, \tag{13}$$

which is derived for the relation between the excitation and de-excitation rates for a suitable approximation of the cross section (see Appendix).

We assume that the χ particles have decoupled from the radiation at a much earlier time than is relevant for the freeze-out of the excited states, i.e. $T_{\rm dec} \gg \delta$; the kinetic temperature T and the photon temperature T_γ are then related by $T_\gamma \approx \sqrt{T_{\rm dec}T}$. The kinetic temperature evolves as

$$\frac{dT}{dt} = -2H(t)T - \frac{2\delta}{3}[k_E n_\chi - k_D n_{\chi^*}]. \quad (14)$$

The first term describes the adiabatic cooling of the WIMPs, while the second is the thermal energy absorbed and injected as the WIMPs excite and de-excite. This implicitly assumes that the elastic scattering cross section is much greater than the excitation/de-excitation cross sections; this ensures that the kinetic energy gained/lost through de-excitations/excitations is efficiently thermalized and the χ particles maintain a Boltzmann distribution. Comparing the right-hand side of Eq. (11) and (14), it is possible to simplify Eq. (14) and obtain

$$\frac{d(x^{-1})}{dt} + \frac{2H(t)}{x} = -\frac{2}{3}\frac{dY}{dt}. \quad (15)$$

Substituting $\ln(\tilde{a}) \equiv \ln(a/a_{\rm dec})$ for the time variable, where $a_{\rm dec}$ is the scale factor at kinetic decoupling, yields the following coupled Boltzmann equations:

$$\frac{dx}{d\ln\tilde{a}} = 2x + \frac{2x^2}{3}\frac{dY}{d\ln\tilde{a}}, \quad (16)$$

and from Eq. (12),

$$\frac{dY}{d\ln\tilde{a}} = -\frac{\alpha_{\rm dec}}{4\tilde{a}}\sqrt{\frac{x_{\rm dec}}{x}}[Y - (1-Y)f(x)e^{-x}], \quad (17)$$

where $\alpha_{\rm dec} \equiv k_D(a_{\rm dec})n(a_{\rm dec})/H(a_{\rm dec})$. Using our fiducial cosmology, we estimate $\alpha_{\rm dec}$

$$\alpha_{\rm dec} \sim 10^8 \tilde{\sigma}_{mr} \times \left(\frac{T_{\rm dec}}{1\ {\rm GeV}}\right)^{3/2}\left(\frac{M_\chi}{100\ {\rm GeV}}\right)^{-5/2} \times \left(\frac{\delta}{1\ {\rm MeV}}\right)^{-1}. \quad (18)$$

The evolution of the excited fraction with time (Fig. 3) exhibits the expected features: $Y = 1/2$ until the temperature reaches $\sim\delta$, after which time it rapidly falls until the Hubble expansion shuts off the de-excitation reactions, and it asymptotes to its freeze-out value, Y_f. We also observe that the modifications to the simplest formulation—the difference between k_E and k_D, and the change in the gas temperature due to the changing fraction of χ in the excited state—have comparable effects on the freeze-out abundance. Plotting Y_f as a function of various XDM parameters (Fig. 4), we find that a significant residual fraction can survive in some cases, though Y_f is smaller for parameters favored by the INTEGRAL signal [1,2], as computed in [3].

While it is convenient to use $\alpha_{\rm dec}$ and $x_{\rm dec}$ to define the initial conditions, there is an alternative which yields a useful scaling of Y_f with $\alpha_{\rm dec}$ and $x_{\rm dec}$. To derive this, we start by noting that the combination $c = (\alpha_{\rm dec}/\tilde{a})\sqrt{x_{\rm dec}/x}$ (which compares the de-excitation rate to the Hubble expansion) controls the behavior of the system. While $c \gg 1$, Y remains at its equilibrium value, and the kinetic

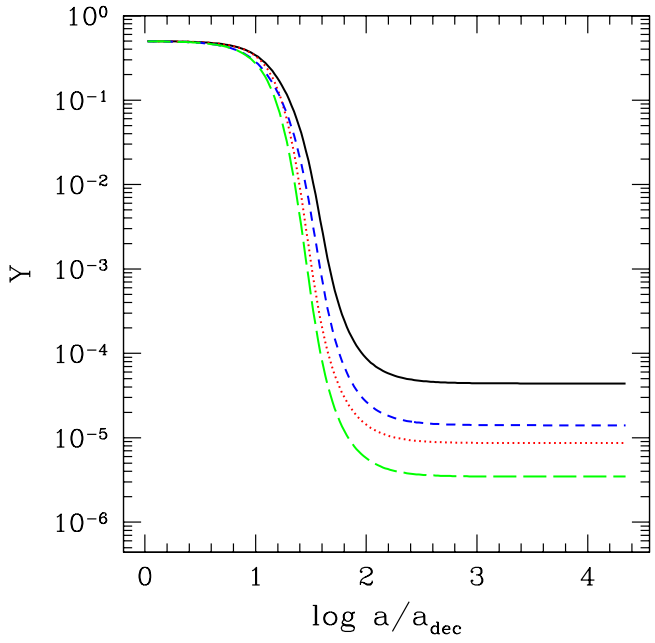

FIG. 3 (color online). The evolution of the excitation fraction with time, for $M_\chi = 1$ TeV, $T_{\rm dec} = 100$ MeV, $\delta = 1$ MeV, and $\tilde{\sigma}_{mr} = 1$ (see Eq. (A11)). Solutions are shown for the full coupled Boltzmann equations (solid black). We show the results under certain additional approximations as well, in particular, with temperature coupling turned off (dashed blue), for the approximation $k_E = k_D \exp(-\delta/T)$, ignoring the corrections in the Appendix (red dotted), and for temperature coupling turned off *and* $k_E = k_D \exp(-\delta/T)$ (long-dashed green).

temperature simply evolves as a^{-2}. This suggests defining the initial condition as the epoch when $c = c_0 \gg 1$. This occurs when $\tilde{a}^2 = \alpha_{\rm dec}/c_0$, or when $x_0 = x_{\rm dec}\alpha_{\rm dec}/c_0$. If $x_0 \ll 1$, then Eqs. (16) and (17) will have identical initial starting points if $\alpha_{\rm dec}x_{\rm dec}$ is the same, as c_0 is just an arbitrary constant. This implies that the freeze-out value only depends on the combination $\alpha_{\rm dec}x_{\rm dec}$. This will not be true if $x_0 > 1$, but in this case, the system will remain in equilibrium as the temperature falls below δ, and the residual fraction will be exponentially suppressed to an uninteresting value. The combination $\alpha_{\rm dec}x_{\rm dec}$ scales with the XDM parameters as

$$\alpha_{\rm dec}x_{\rm dec} = 10^5 \tilde{\sigma}_{mr}\left(\frac{T_{\rm dec}}{1\ {\rm GeV}}\right)^{1/2}\left(\frac{M_\chi}{100\ {\rm GeV}}\right)^{-5/2}. \quad (19)$$

Interestingly, it is independent of δ, at least for the assumption of $T_{\rm dec} \gg \delta$ made above. This relationship provides a better understanding of the scaling of the curves in Fig. 4. In spite of the exponential uncertainty in the relic excitation, it is natural to have significant and interesting relic excitation fractions. Thus, we now turn to the observable consequences of such a large Y_f.

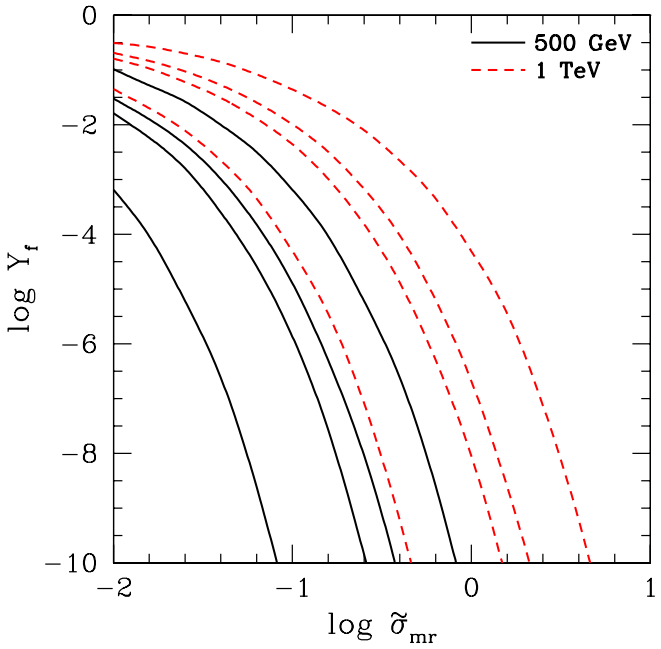

FIG. 4 (color online). The residual excitation fraction Y_f as a function of the scattering cross section $\tilde{\sigma}_{mr}$, and decoupling temperature $T_{\rm dec}$, for $M_\chi = 500$ GeV (solid black) and $M_\chi = 1$ TeV (dashed red). From top to bottom for each mass, the decoupling temperatures are $T_{\rm dec} = 100$ MeV, 500 MeV, 1 GeV, and 10 GeV. The 511 keV signal favors $\tilde{\sigma}_{mr} = 0.1$–50 for a 500 GeV WIMP.

IV. OBSERVATIONAL SIGNATURES

In this section, we consider the consequences of WIMP de-excitation at early enough times ($z > 10$) that the collisional excitation and de-excitation expected for centers of halos at late times is unimportant.

The most obvious observables affected by energy injection into the intergalactic medium during the "dark ages" ($10 < z < 500$) are the cosmic microwave background (CMB) and the high-z 21 cm background. The effect of DM annihilations and decays on the CMB has previously been discussed [10–12]; the case at hand is more like DM decay. The energy injection from WIMP decay, whether from sterile neutrinos [13], superheavy dark matter [14], or generically [15], has been shown to affect the ionization history [16], though if the lifetime of the decaying particle is longer than the age of the Universe, perturbations to the CMB power spectrum are small [12,17]. Effects on the high-z 21 cm [18,19] and structure formation [20] have also been investigated. As we shall see, the XDM WIMP exhibits a much larger range of observable signals for natural models, in part, because a potentially large fraction of the DM can participate, but also because the characteristic energy scales are significantly lower and can be absorbed efficiently by the gas.

We begin by estimating the relevant time scales for energy deposition, and demonstrate that the $e^\pm$ pairs produced by XDM de-excitations deposit their kinetic energy efficiently. We then consider the possible consequences of this energy deposition and the potential for detecting it in current and future experiments.

A. Energy deposition timescales

The de-excitation of χ^* deposits energy into the intergalactic medium in the form of nonrelativistic electron-positron pairs with kinetic energies $\sim$100 keV. The dominant energy loss for such electrons is via collisions, with a cross section for collisional ionization [21] of

$$\sigma_{eH} = \frac{2.23 \times 10^{-15} \ln(E/13.6)}{E} \ {\rm cm}^2, \qquad (20)$$

where E is the kinetic energy in eV. The cross sections for excitations and heating are similar. For a 100 keV electron, this corresponds to a cross section of $\sim 2 \times 10^{-19}$ cm^2, or a scattering rate of

$$n_H \sigma_{eH} v \sim 5 \times 10^{-13} \left(\frac{1+z}{10}\right)^3 \ {\rm s}^{-1}. \qquad (21)$$

Comparing this to the Hubble time

$$\frac{1}{H(z)} \sim 10^{16} h^{-1} \left(\frac{1+z}{10}\right)^{-3/2} \ {\rm s} \qquad (22)$$

we see that collisional energy deposition is extremely efficient over the entire redshift range of interest. We assume that all the kinetic energy of the electrons is instantaneously partitioned between ionizations, heating, and excitations.

The above has focused on the deposition of the kinetic energy of the $e^\pm$ pairs; there is an additional $\sim$1 MeV available from the rest mass energy of $e^\pm$. Positrons can annihilate to 2 photons at 511 keV, or to 3 photons. The 3γ spectrum of ortho-positronium [22] is very hard, with only 7×10^{-3} of the power coming out at $E_\gamma < 100$ keV and 7×10^{-6} at $E_\gamma < 10$ keV. At redshift $z < 100$, the Universe is nearly transparent to these photons, so their energy is effectively lost. At $z > 100$ the photon energy density is high enough that Compton scattering happens faster than a Hubble time, so for relevant lifetimes ($\tau_{\chi^*} \approx 10^{13}$–$10^{14}$ s) the mass energy of the pair must be included (see e.g. [23]), giving rise to a higher effective η.

B. Ionization/thermal history

The effects of XDM on the ionization and thermal history of the Universe are controlled by two parameters—the available energy per baryon ϵ_b and the lifetime of the excited state τ_{χ^*}. The energy per baryon is determined both by the energy splitting δ and the residual excitation fraction Y_f

$$\epsilon_b = Y_f \frac{n_\chi}{n_b}(\delta - 2m_e c^2), \qquad (23)$$

where the $n_{b,\chi}$ are the number densities of baryons and

XDM particles. To more easily connect to the relic abundance calculation of the previous section, we fix $\delta - 2m_e c^2$ to 100 keV and n_χ/n_b to 10^{-2} below, corresponding to a WIMP mass of 500 GeV. The energy per baryon is then trivially related to the relic abundance by

$$\epsilon_b \approx 10^3 Y_f \text{ eV}, \tag{24}$$

allowing us to express our results in terms of Y_f and τ_{χ^*}. It is straightforward to relate the results below to cases that make different assumptions for the energy splitting and number densities.

We modify the publicly available code `RecFast` [24] to numerically calculate the ionization and thermal histories [25,26]. Examples of these for different choices of XDM parameters are plotted in Figs. 5 and 6 where we hold one parameter fixed and vary the other.

The effect of varying Y_f at constant lifetime is as one expects, with an increasing ionization fraction and temperature as Y_f, and therefore ϵ_b, increases. The dependence on the lifetime is more involved. For lifetimes much shorter than the age of the Universe at recombination ($\tau_{\chi^*} \ll 10^{13}$ s), the energy is simply injected into a fully ionized medium with no effect. Injecting energy soon after recombination $\tau_{\chi^*} \sim 10^{14}$ s can truncate recombination early, resulting in a higher residual ionization level. For

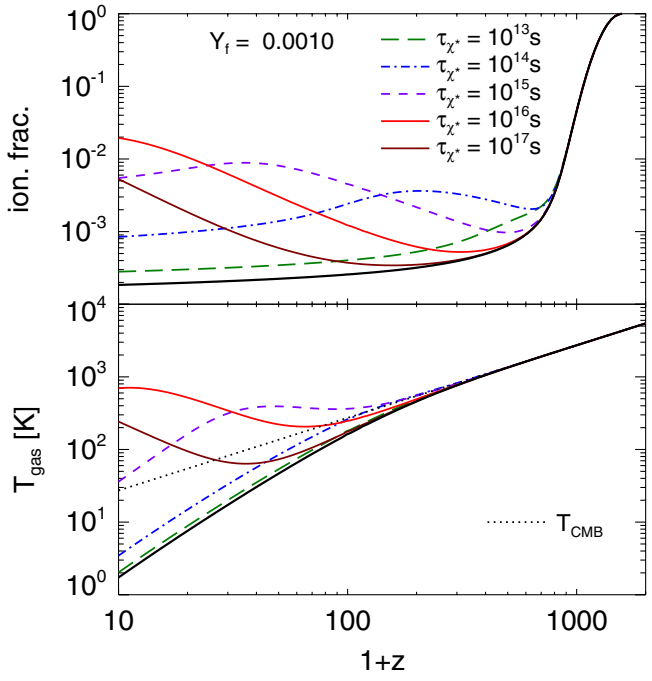

FIG. 5 (color online). The ionization fraction $x_i \equiv n(e^-)/n(H)$ (*top*), and matter temperature (bottom), for various values of the lifetime, τ_{χ^*}, with Y_f held fixed. The baseline scenario, with no energy injection from WIMPs, is shown in both panels (thick solid line), and T_{cmb} is included in the bottom panel (dotted line). In all cases we take $Y_f = 10^{-3}\epsilon_b$. Note that we ignore the effects of star formation, etc. on the ionization fraction and temperature.

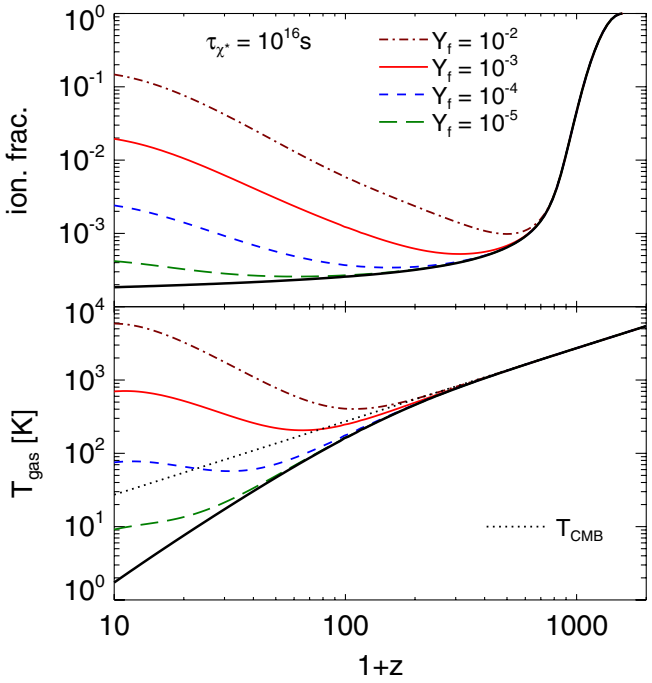

FIG. 6 (color online). Same as Fig. 5, but for various values of Y_f with $\tau_{\chi^*} = 10^{16}$ s. The fiducial model ($Y_f = 10^{-3}$ and $\tau_{\chi^*} = 10^{16}$ s) is represented by a thin solid line in both figures.

even longer lifetimes, the injected energy does not perturb the baseline recombination, but partially re-ionizes the Universe. However, unlike the previous case, the recombination processes have been shut off by the Hubble expansion, and so the ionization fraction monotonically increases with time. This behavior qualitatively persists for longer lifetimes, but the degree of reionization decreases as τ_{χ^*} becomes a significant fraction of the age of the Universe today, and there simply has not been enough time for the χ^* to de-excite.

The gas temperature behaves similarly, except that it remains thermally locked to the photon temperature until $z \sim 300$, much later than recombination. Lifetimes shorter than this have little effect on the gas temperature.

The above has concentrated on the homogeneous universe—the formation of collapsed halos could modify this in two ways. The first is the $\chi - \chi^*$ collisions could de-excite the χ^*. Such de-excitations only increase the kinetic energy of the colliding WIMPs and do not inject energy into the IGM. The second effect occurs when virial motions inside halos can re-excite the dark matter. This only happens for halos with velocities $> \sqrt{\delta/M_\chi}$ and only becomes significant after the ionization and temperature have already been considerably modified by star formation.

C. Implications for CMB and 21-cm observations

The only two probes of the $z > 10$ ionization and thermal history of the Universe are the CMB and the measure-

ments of the 21-cm hyperfine splitting in hydrogen. While CMB measurements are now a mature field, they are less constraining because they are only sensitive to the integrated ionization history and do not probe the temperature of the IGM. On the other hand, 21-cm measurements probe both the temperature and ionization as a function of time, but the experimental techniques are less developed with the first pathfinder experiments scheduled for the near future. We consider both of these in turn below.

1. CMB power spectrum

The polarization anisotropy of the CMB, and its correlation with the temperature anisotropy, can provide a powerful constraint on the ionization history of the Universe. The CMB polarization is principally induced by Thomson scattering [27], and was first observed on small scales by the DASI interferometer [28], and on large scales by the WMAP [29]. The small-scale polarization is sensitive to ionization at the epoch of recombination, while large-scale measurements probe the epoch of reionization at $z \approx 10$. Such data are, in principle, sensitive to any perturbation of the ionization history of the Universe caused by new physics, such as XDM.

The effect of XDM on the CMB may be conceptually separated into two regimes—effects on recombination ($\tau_{\chi^*} \sim 10^{14}$ s) and effects on reionization ($\tau_{\chi^*} \sim 10^{16}$ s). The dominant effect on recombination may be thought of as an increased residual fraction of ionized atoms, which broadens the surface of last scattering. The increased scattering both washes out the temperature fluctuations, and enhances and shifts the polarization power spectra. These effects on the CMB were discussed in detail by [11] for the case of WIMP annihilation, but the basic physics is also relevant here. Figure 7 plots the temperature and polarization power spectra for two examples of XDM parameters, with the lifetime chosen to highlight the effects on recombination. While the differences in the temperature-temperature power spectrum are degenerate with the slope of the primordial power spectrum, these degeneracies are mostly broken by the polarization power spectra. Figure 7 also plots the nominal polarization sensitivities of current and future CMB measurements.

The detectability of these changes in the power spectrum will depend on many factors, including degeneracies with other cosmological parameters and details of reionization. Nevertheless, we may estimate constraints on the $z \approx 1000$ energy injection. The limit on such energy injection, marginalizing over the usual cosmological parameters, is $\epsilon_{\rm DM} < 3 \times 10^{-14}$ from WMAP, with an improved limit of $\epsilon_{\rm DM} < 10^{-15}$ eV/s/baryon at $z = 1000$ expected from Planck [11]. Using Eq. (3) for $\eta = 2 \times 10^{-7}$ we have

$$\epsilon_{\rm DM} = 10^3 Y_f / \tau_{\chi^*} \text{ eV/s/baryon} \tag{25}$$

yielding constraints of

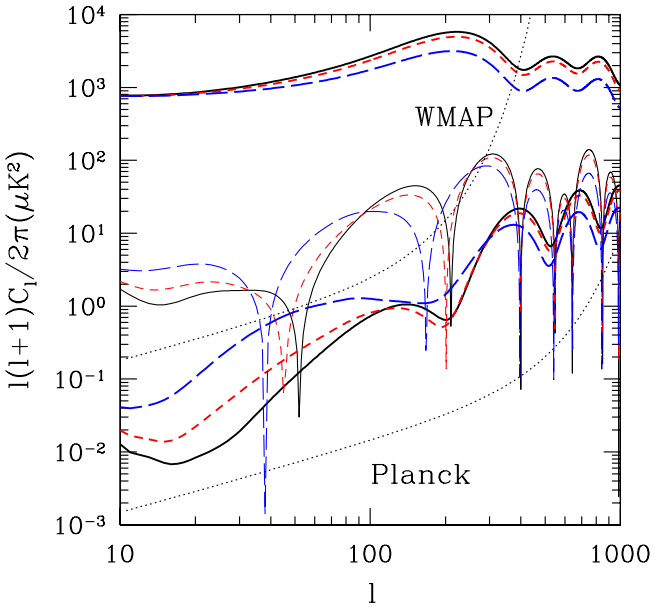

FIG. 7 (color online). The effect of XDM on the CMB temperature-temperature, TE, and EE power spectra. The solid (black) line is our fiducial cosmology, with no XDM. The short-dashed (red) line assumes XDM with $Y_f = 10^{-3}$, $M_\chi = 500$ GeV, $\delta = 1.1$ MeV, and $\tau_{\chi^*} = 10^{14}$ s, while the long-dashed line assumes $Y_f = 10^{-2}$ with the other parameters the same. For lifetimes much less than 10^{13} s, the de-excitation of XDM has a negligible effect on the CMB, since the Universe is already completely ionized. For decays much later, the dominant effect is only on the largest scales, and therefore hard to disentangle from standard reionization. Also plotted are nominal curves for the polarization sensitivity in bins of $\log_{10}(\ell) = 0.05$ for the WMAP and Planck CMB missions. Uncertainty due to cosmic variance is not included in these sensitivity estimates.

$$\begin{aligned} Y_f &< 3 \times 10^{-4} (\tau_{\chi^*}/10^{13} \text{ s}) \quad \text{WMAP} \\ Y_f &< 10^{-5} (\tau_{\chi^*}/10^{13} \text{ s}) \quad \text{Planck.} \end{aligned} \tag{26}$$

These constraints do not include higher ℓ data from e.g. ACBAR [30] and CBI [31]. Using the ϵ_α parametrization for delayed recombination in (defined by Peebles *et al.* [10]) Kim and Naselsky find that $\epsilon_\alpha < 0.02$ based on WMAP and ACBAR [32]. This constraint also converts to $Y_f < \sim 2 \times 10^{-4} (\tau_{\chi^*}/10^{13} \text{ s})$ in agreement with Eq. (26).

For longer lifetimes $\tau_{\chi^*} > 10^{15}$ s, the effect on the reionization history ($z \approx 10$) could be pronounced. In this limit, it is useful to express the information in the CMB polarization in the form of a scattering optical depth, τ, given by

$$\tau = \frac{n_0 \sigma_T c}{H_0} \int_{a_{\rm ref}}^1 \frac{da}{a^4} \frac{x_i(a)}{\sqrt{\Omega_m/a^3 + \Omega_\Lambda}}, \tag{27}$$

where n_0 is the number density of H at $z = 0$, x_i is the ionized fraction of H, $a_{\rm ref}$ is the scale factor at some early

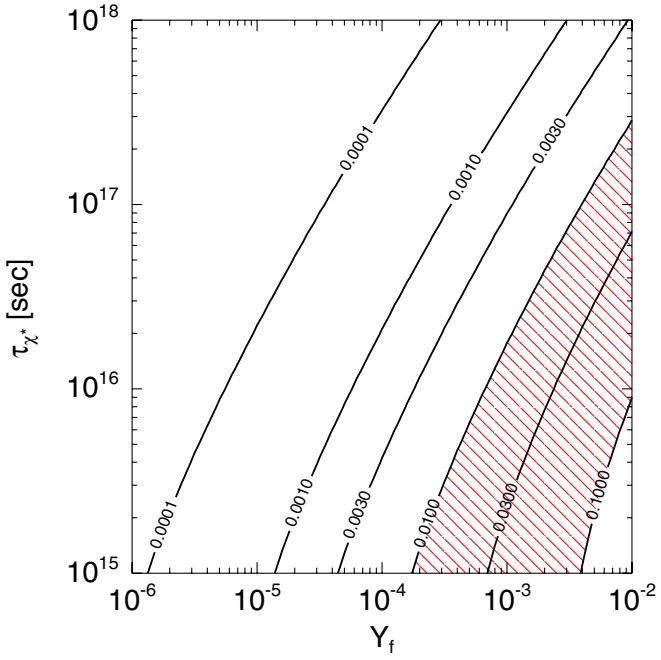

FIG. 8 (color online). The *excess* optical depth for CMB scattering, $\Delta\tau$ (see Sec. IV C 1). The hatched region is accessible to observation, with $\Delta\tau > 0.1$ already ruled out by CMB observations, and $\Delta\tau < 0.01$ difficult to notice in the presence of the reionization caused by standard astrophysics.

reference time, and the Hubble parameter has been expressed in terms of H_0, Ω_m, and Ω_Λ. We are interested in the "excess" optical depth due to χ^* decay, $\Delta\tau = \tau(Y_f, \tau_{\chi^*}) - \tau(Y_f = 0)$, which we compute for a range of Y_f and τ_{χ^*} (Fig. 8). We identify the region of parameter space where $\Delta\tau$ is large enough to distinguish from the somewhat uncertain standard scenario ($\Delta\tau \sim 0.01$) and small enough to be ruled out by WMAP ($\Delta\tau \sim 0.1$). While the CMB is a good probe of relic XDM excitation in some parts of parameter space, 21-cm experiments have a broader reach.

2. 21 cm observations

The hyperfine (spin-flip) transition in neutral atomic hydrogen provides a source of opacity to the cosmic microwave background from the time the gas temperature decouples from the CMB ($z = 200$) until reionization ($z \sim$ 10–20). In the standard scenario, $T_S < T_\gamma$ and the line appears in absorption. If sufficient energy is injected by new physics (or any other mechanism) such that $T_S > T_\gamma$, the line will appear in emission. Observations of this line have the potential to constrain the evolution of the matter power spectrum, and reveal new information about the first sources of ionizing radiation [12,18,33]. Several projects are already underway to observe the line at $z \sim 7$–14 (e.g. the Murchison Widefield Array [34], LOFAR [35], and others). The heroic observing efforts now underway may be sensitive to the expected signal from relic XDM excitation within 5–10 years.

Following standard practice, we assume the spin temperature T_S is well defined in each volume element of space, and neglect the subtle variation of T_S with atomic velocity [36] needed for high-precision calculations. We relate T_S to the ratio of the number densities of ground state and excited atoms via

$$\frac{n_1}{n_0} = \frac{g_1}{g_0} \exp\left(\frac{-T_*}{T_S}\right), \tag{28}$$

where $g_1/g_0 = 3$ is the degeneracy factor, and $T_* = 0.068$ K is the temperature corresponding to the energy of the transition.

The mean (sky-averaged) signal $\delta\bar{T}_b$ is given by

$$\delta\bar{T}_b = 27(1 - x_i)\left(\frac{1+z}{10}\right)^{1/2}\left(\frac{T_S - T_\gamma}{T_S}\right) \text{ mK}, \tag{29}$$

where x_i is the ionization fraction, standard cosmological parameters are assumed, and radial peculiar velocity of the gas is neglected [18]. Figures 10 and 11 show $\delta\bar{T}_b$ for the same set of parameters as Figs. 5 and 6.

Computation of the T_S history involves collisional coupling of T_S to T_K via both H-H and H-e^- collisions [18,37,38]. Another important effect is the Wouthuysen-Field coupling, in which photons in the Ly α resonance region exchange energy with atoms via Doppler shift, and also couple to the hyperfine transition via Raman scattering [39–41]. The net result is that the presence of Ly α photons more tightly couples T_S to the gas temperature. We follow

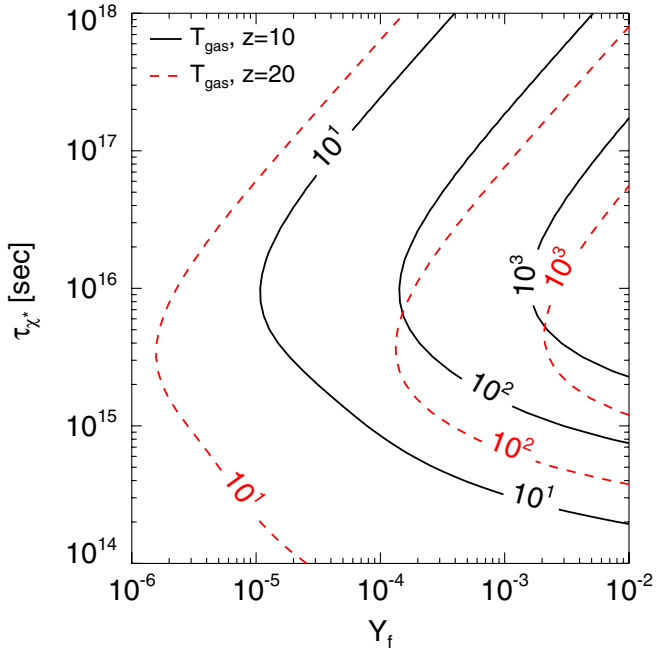

FIG. 9 (color online). The gas temperature [K] as a function of the freeze-out excitation fraction Y_f, and the lifetime τ_{χ^*}, for two redshifts.

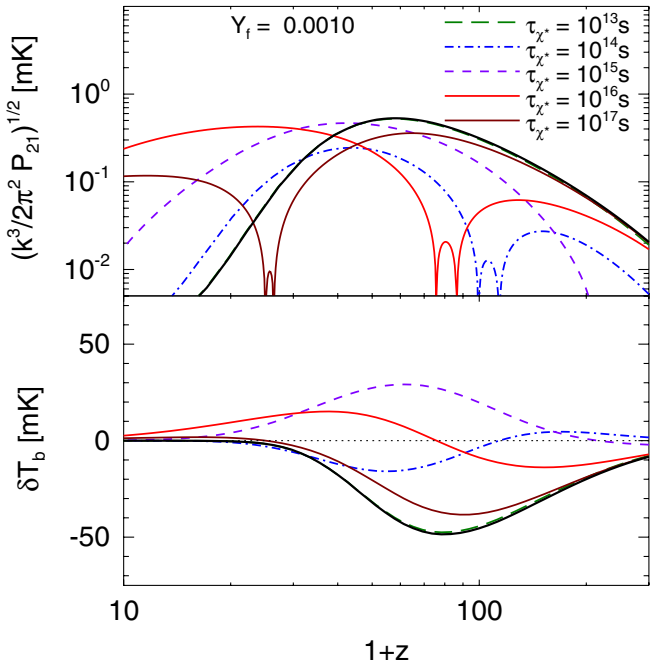

FIG. 10 (color online). 21 cm signals: the fluctuation amplitude for an arbitrary scale, $k = 0.04\ \mathrm{Mpc}^{-1}$ (top), and mean (sky-averaged) signal (bottom), for various values of the lifetime, τ_{χ^*}, with Y_f held fixed. The baseline scenario, with no energy injection from WIMPs, is shown in both panels (thick solid line), and $\delta T_b = 0$ is shown in the bottom panel (dotted line). In all cases, we take $Y_f = 10^{-3}\epsilon_b$. Line styles and colors are the same as Fig. 5 for easy comparison.

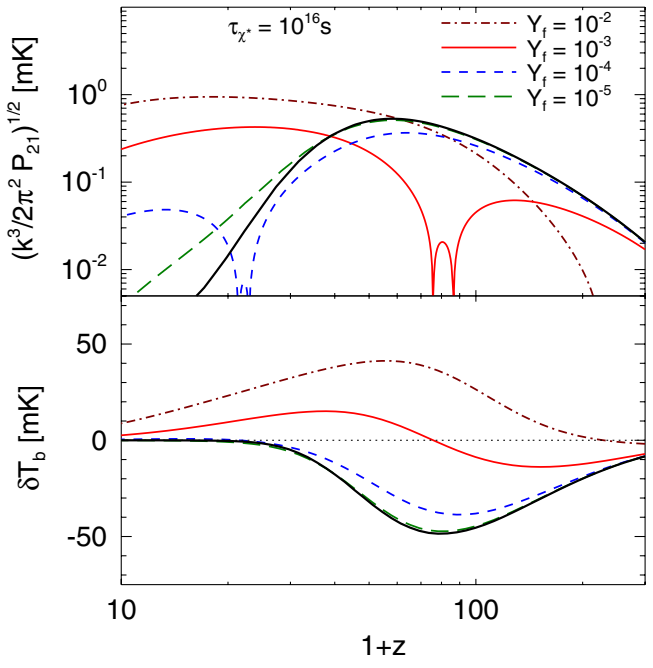

FIG. 11 (color online). Same as Fig. 10 but for various values of Y_f with $\tau_{\chi^*} = 10^{16}$ s. The fiducial model ($Y_f = 10^{-3}$ and $\tau_{\chi^*} = 10^{16}$ s) is represented by a red solid line in both figures.

standard procedure [18,33] to compute T_S and the gas temperature, T_K (Fig. 9).

Because the galactic synchrotron foreground is orders of magnitude brighter than $\delta\bar{T}_b$, the more relevant signal to consider is the signal from fluctuations in the gas density. These fluctuations cause the observed signal to vary both because the density of the gas (and therefore optical depth) varies, and also the ionization state and temperature. Following [18], we combine these effects and present the expected amplitude at wavenumber $k = 0.04\ \mathrm{Mpc}^{-1}$ (Figs. 10 and 11). This scale is arbitrary, but is chosen to be roughly the largest scale observable by the current generation of arrays. It is clear that at $z \sim 10$ XDM energy injection could provide a substantial enhancement over the baseline scenario. However, the first stars or other astrophysical sources could also produce a dramatic signal, so mapping the history at higher z would be necessary to unambiguously identify any new physics.

V. CONCLUSIONS

XDM was invented to explain the 511 keV signal in the center of the Milky Way. This was achieved by converting WIMP kinetic energy into excitations, and then into $e^{\pm}$ pairs from subsequent decays. An unintended feature of XDM is that the lifetime of the excited state τ_χ^* may be long ($\sim 10^{13}$–10^{18} s). We have computed the expected relic excitation fraction Y_f left over from the early Universe, and explored a variety of observable consequences for various Y_f values and lifetimes.

Such features would be generic in a wide class of models with excited states, beyond the simple model of [3]. We find that for the parameters that explain the 511 keV signal (500 GeV mass, $\tilde{\sigma}_{mr} \approx 0.1$–50) the expected Y_f is small. However, for a higher mass particle and weaker cross section, very substantial relic densities (up to $Y_f = 10^{-2}$) are possible, which may be generic in models with multiple excited states. The thermal, ionization, and spin temperature histories of the Universe are sensitive tests of the detailed physics of dark matter properties, to which collider tests may be insensitive. Upcoming probes of this era may show anomalies, giving essential insight into the nature of dark matter.

ACKNOWLEDGMENTS

D. P. F. is partially supported by NASA LTSA Grant No. NAG5-12972. N. P. is supported by NASA Hubble Contract No. HST-HF-01200.01 and the Space Telescope Science Institute, which is operated by the Association of Universities for Research in Astronomy, Inc., for NASA, under Contract No. NAS 5-26555. N. P. is also supported by LBNL. This work was partially supported by the Director, Office of Science, of the U.S. Department of Energy under Contract No. DE-AC02-05CH11231. N. W. is supported by NSF CAREER Grant No. PHY-0449818

and DOE OJI Grant No. DE-FG02-06E R41417. We thank an anonymous referee for helpful comments on the current CMB constraints. We are grateful to the Stanford Physics Department for hospitality at the inception of this project.

APPENDIX: ESTIMATING (DE-)EXCITATION RATES

The velocity excitation/de-excitation rate coefficients (k_D, k_E; scatterings per time per density) are given by

$$k_{D,E}(\mathbf{r}) = \int d^3v_1 d^3v_2 f(\mathbf{v}_1, \mathbf{r}) f(\mathbf{v}_2, \mathbf{r}) \sigma_{D,E}(v_{\rm rel}) v_{\rm rel}, \tag{A1}$$

where $f(\mathbf{v}, \mathbf{r})$ is the phase-space density of particles with velocity $\mathbf{v}$ at position $\mathbf{r}$, $\sigma_{D,E}(v_{\rm rel})$ is the inelastic scattering cross section as a function of the relative velocity $v_{\rm rel} = |\mathbf{v}_1 - \mathbf{v}_2|$. Assuming the Universe is homogeneous and the particles are nonrelativistic, the phase-space density is given by the Maxwell-Boltzmann distribution

$$f(\mathbf{v}, \mathbf{r}) = \left(\frac{m}{2\pi T}\right)^{3/2} \exp\left(\frac{-mv^2}{2T}\right), \tag{A2}$$

where m is the mass of the particle, and T is the kinetic temperature (in energy units). It is convenient to transform to center of mass variables, $\mathbf{V}_{\rm cm}$ and $\mathbf{v}_{\rm rel}$, which decouples the velocity integrals over both particles,

$$k_{D,E} = \left(\frac{m}{4\pi T}\right)^{3/2} \int d^3v_{\rm rel} \exp\left(\frac{-mv_{\rm rel}^2}{4T}\right) \sigma(v_{\rm rel}) v_{\rm rel}. \tag{A3}$$

If, following [3], we assume the de-excitation cross section, σ_{mr}, is independent of velocity, we obtain for the de-excitation rate,

$$k_D = 4\sigma_{mr}\sqrt{\frac{T}{\pi m}}. \tag{A4}$$

which scales as $\sqrt{T}$ as expected from dimensional arguments. We approximate the excitation rate (Eq. (2) of [3]) with

$$\begin{aligned} \sigma v_{\rm rel} &= \sigma_{mr}\sqrt{v_{\rm rel}^2 - 4\delta/m} \quad v_{\rm rel}^2 \geq 4\delta/m \\ &= 0 \quad v_{\rm rel}^2 < 4\delta/m, \end{aligned} \tag{A5}$$

where δ is the energy splitting between χ and χ^*, and we assume the same (velocity-independent) cross section, σ_{mr} as for de-excitation. Setting $x = v_{\rm rel}\sqrt{m/4T}$ yields

$$k_E = 2k_D \int_{\sqrt{\delta/T}}^{\infty} dx x^2 e^{-x^2} \sqrt{x^2 - \delta/T}. \tag{A6}$$

Changing variables,

$$k_E = k_D \int_{\delta/T}^{\infty} dy \sqrt{y} e^{-y} \sqrt{y - \delta/T}, \tag{A7}$$

which is a known integral (Eq. 3.383 of [42]) giving

$$k_E = k_D\left(\frac{\delta}{2T}\right) K_1\left(\frac{\delta}{2T}\right) \exp\left(\frac{-\delta}{2T}\right), \tag{A8}$$

where K_1 is the modified Bessel function of the second kind. Using the fact that $zK_1(z) \approx 1$ as $z \to 0$, we see that $k_E \approx k_D$ for $T \gg \delta$. As $T \ll \delta$, we find

$$k_E \sim k_D \sqrt{\frac{\pi\delta}{4T}} \exp\left(\frac{-\delta}{T}\right). \tag{A9}$$

This implies that k_E decreases slower than the naive Boltzmann scaling suggests, although the correction only grows as $\sqrt{\delta/T}$. The asymptotic expressions suggest an approximation,

$$k_E \approx k_D \sqrt{\left(1 + \frac{\pi\delta}{4T}\right)} \exp\left(\frac{-\delta}{T}\right); \tag{A10}$$

this approximation agrees with Eq. (A8) to within a few percent for $T > \delta$.

Finally, it is useful to estimate a numerical value for these rate coefficients. As in [3], we assume σ_{mr} is determined by the momentum transfer, $\sigma_{mr} = \tilde{\sigma}_{mr}/\delta m$, where $\tilde{\sigma}_{mr}$ is assumed to be independent of δ and m. Choosing fiducial values, this gives

$$\begin{aligned} k_D \sim 2\tilde{\sigma}_{mr}\ {\rm GeV}^{-2} &\left(\frac{\delta}{1\ {\rm MeV}}\right)^{-1} \left(\frac{T}{1\ {\rm GeV}}\right)^{1/2} \\ &\times \left(\frac{m}{100\ {\rm GeV}}\right)^{-3/2}, \end{aligned} \tag{A11}$$

with $1\ {\rm GeV}^{-2} = 3.90 \times 10^{-28}\ {\rm cm}^2$.

[1] G. Weidenspointner *et al.*, Astron. Astrophys. **450**, 1013 (2006).
[2] G. Weidenspointner *et al.*, arXiv:astro-ph/0702621.
[3] D. P. Finkbeiner and N. Weiner, Phys. Rev. D **76**, 083519 (2007).
[4] C. Boehm, D. Hooper, J. Silk, M. Cassé, and J. Paul, Phys. Rev. Lett. **92**, 101301 (2004).
[5] J. F. Beacom, N. F. Bell, and G. Bertone, Phys. Rev. Lett. **94**, 171301 (2005).
[6] J. F. Beacom and H. Yuksel, Phys. Rev. Lett. **97**, 071102 (2006).
[7] M. Pospelov and A. Ritz, Phys. Lett. B **651**, 208 (2007).

[8] It is possible that the vacuum expectation value of ϕ could be smaller than m_ϕ if there are other sources of symmetry break generating the splitting between χ and χ^*. Such effects could even be beneficial for early Universe cosmology [3]. If such effects are present, they could also contribute to the mixing of ϕ, for instance through terms such as $A\phi h^\dagger h$. Nonetheless, such terms should be related to m_ϕ through radiative corrections, and we expect the scaling of the mixing angle with m_ϕ to be fairly robust in a wide variety of theories.
[9] J. F. Gunion, H. E. Haber, G. L. Kane, and S. Dawson (1989), the Higgs Hunter's Guide, SCIPP-89/13.
[10] P. J. E. Peebles, S. Seager, and W. Hu, Astrophys. J. **539**, L1 (2000).
[11] N. Padmanabhan and D. P. Finkbeiner, Phys. Rev. D **72**, 023508 (2005).
[12] M. Mapelli, A. Ferrara, and E. Pierpaoli, Mon. Not. R. Astron. Soc. **369**, 1719 (2006).
[13] S. H. Hansen and Z. Haiman, Astrophys. J. **600**, 26 (2004).
[14] A. G. Doroshkevich and P. D. Naselsky, Phys. Rev. D **65**, 123517 (2002).
[15] R. Bean, A. Melchiorri, and J. Silk, Phys. Rev. D **68**, 083501 (2003).
[16] E. Pierpaoli, Phys. Rev. Lett. **92**, 031301 (2004).
[17] X.-L. Chen and M. Kamionkowski, Phys. Rev. D **70**, 043502 (2004).
[18] S. Furlanetto, S. P. Oh, and E. Pierpaoli, Phys. Rev. D **74**, 103502 (2006).
[19] M. Valdes, A. Ferrara, M. Mapelli, and E. Ripamonti, Mon. Not. R. Astron. Soc. **377**, 245 (2007).
[20] E. Ripamonti, M. Mapelli, and A. Ferrara, Mon. Not. R. Astron. Soc. **375**, 1399 (2007).
[21] J. M. Shull and M. E. van Steenberg, Astrophys. J. **298**, 268 (1985).
[22] A. Ore and J. L. Powell, Phys. Rev. **75**, 1696 (1949).
[23] E. Ripamonti, M. Mapelli, and A. Ferrara, Mon. Not. R. Astron. Soc. **374**, 1067 (2007).
[24] http://www.astro.ubc.ca/people/scott/recfast.html.
[25] S. Seager, D. D. Sasselov, and D. Scott, Astrophys. J. Lett. **523**, L1 (1999).
[26] S. Seager, D. D. Sasselov, and D. Scott, Astrophys. J. Suppl. Ser. **128**, 407 (2000).
[27] M. J. Rees, Astrophys. J. Lett. **153**, L1+ (1968).
[28] J. Kovac *et al.*, Nature (London) **420**, 772 (2002).
[29] L. Page *et al.* (WMAP), Astrophys. J. Suppl. Ser. **170**, 335 (2007).
[30] C. L. Reichardt *et al.*, arXiv:0801.1491.
[31] J. L. Sievers *et al.*, Astrophys. J. **660**, 976 (2007).
[32] J. Kim and P. Naselsky, Astrophys. J. Lett. **678**, L1 (2008).
[33] A. Loeb and M. Zaldarriaga, Phys. Rev. Lett. **92**, 211301 (2004).
[34] http://www.haystack.mit.edu/ast/arrays/mwa.
[35] http://www.lofar.org.
[36] C. M. Hirata and K. Sigurdson, Mon. Not. R. Astron. Soc. **375**, 1241 (2007).
[37] B. Zygelman, Astrophys. J. **622**, 1356 (2005).
[38] S. R. Furlanetto and M. R. Furlanetto, Mon. Not. R. Astron. Soc. **374**, 547 (2007).
[39] S. A. Wouthuysen, Astron. J. **57**, 31 (1952).
[40] G. B. Field, Astrophys. J. **129**, 536 (1959).
[41] C. M. Hirata, Mon. Not. R. Astron. Soc. **367**, 259 (2006).
[42] I. S. Gradshteyn and I. M. Ryzhik, *Table of Integrals, Series and Products*, edited by, J. Alan (Academic Press, New York, |c1994, completely reset, 1994), 5th ed..